Laser excited luminescence of CaF_2:Ho. The role of phonons

1991 J. Phys.: Condens. Matter 3 5407

(http://iopscience.iop.org/0953-8984/3/28/015)

J. Phys.: Condens. Matter 3 (1991) 5407–5414. Printed in the UK

Laser excited luminescence of CaF_2:Ho. The role of phonons

M Sendova-Vassileva, M Iliev and A V Chadwick†
Faculty of Physics, Sofia University, 1126 Sofia, Bulgaria

Received 13 February 1991

Abstract. The laser excited luminescence of CaF_2:Ho has been studied between 17 and 300 K using various Ar^+ and He–Ne laser lines. The dependence of the effectiveness of excitation on the laser photon energy finds explanation if one-phonon assisted processes are taken into account. The adiabatic model and the model of phonon relaxation has been applied to the experimental linewidth temperature dependence of the A-sites of Ho^{3+} (transition $^5F_4$, $^5S_2 \rightarrow {}^5I_7$) and Er^{3+} (transition $^4S_{3/2} \rightarrow {}^4I_{15/2}$) and the results are discussed.

1. Introduction

The role of lattice phonons in laser excitation and luminescence of trivalent rare-earth ions (RE^{3+}) in CaF_2 was discussed by Iliev *et al* (1988) in an attempt to explain the effectiveness of *indirect* laser excitation of RE^{3+} multiplets and its dependence on laser wavelength and temperature. The particular case of CaF_2:Er^{3+} (for the A-site $^4S_{3/2} \rightarrow {}^4I_{15/2}$ transitions) was studied by Sendova-Vassileva *et al* (1988). The various widths of the emission lines were explained qualitatively in the framework of one-phonon assisted processes taking into account the phonon density of states.

In this work the laser line effectiveness and the temperature evolution of emission linewidths are further studied using experimental results on laser excited luminescence of CaF_2:Ho. The adiabatic approximation (Osad'ko 1979) and the model of phonon relaxation (Yen *et al* 1964) are employed in numerical calculations to analyse the temperature broadening of the luminescence lines. A conclusion is that all the lattice phonons of CaF_2 are involved in the electron–phonon interaction at the A-sites of CaF_2:Ho and CaF_2:Er and the mechanism of one-phonon relaxation between the components of a multiplet is definitely significant for the temperature broadening.

2. Samples and experimental procedure

Two single crystals containing 0.05 and 0.005 at.% Ho were used in our experiments. The samples were cooled in a closed cycle helium cryostat equipped with a thermoregulating unit. The luminescence was excited using the Ar^+ laser lines at 514.5 nm (19435 cm^{-1}), 496.5 nm (20141 cm^{-1}), 488.0 nm (20492 cm^{-1}), 476.5 nm (20987 cm^{-1}) and 457.9 nm

† Department of Chemistry, University of Kent at Canterbury, UK.

0953-8984/91/285407 + 08 $03.50

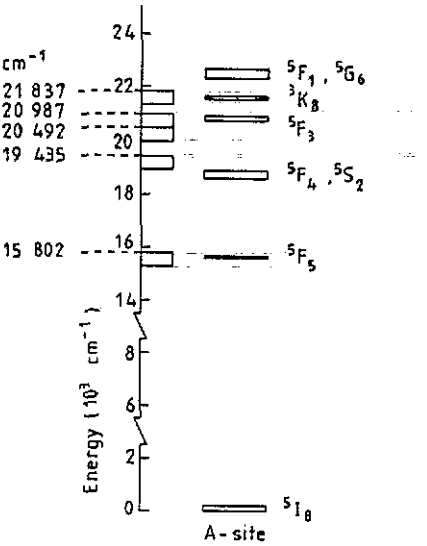

Figure 1. Energy level scheme of A-site of Ho^{3+} in CaF_2 (using data from Seelbinder and Wright, 1979) and the position of the excitation energies with the interval covered by phonon energies in CaF_2 below them.

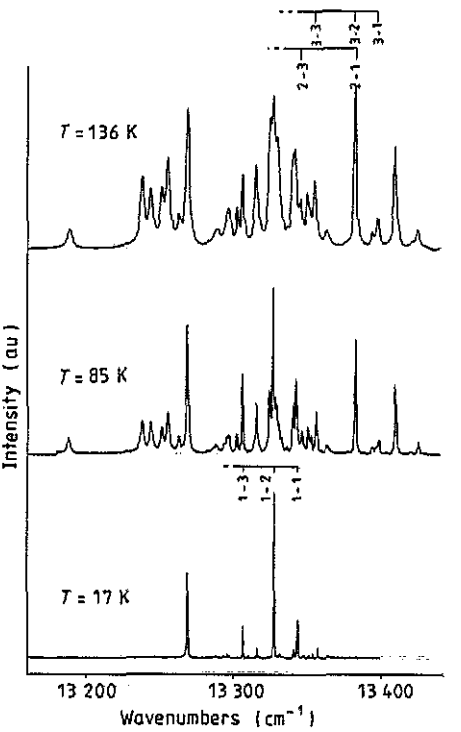

Figure 2. Experimentally observed $^5F_4$, $^5S_2 \rightarrow {}^5I_7$ luminescence of Ho^{3+} in CaF_2 with 476.5 nm excitation at various temperatures.

(21 837 cm^{-1}), and the He–Ne line at 632.8 nm (15 802 cm^{-1}). The emission spectra were recorded by means of a double SPEX 1403 spectrometer and a photon counting system.

3. Experimental results

Figure 1 illustrates that following the model of one-phonon assisted excitation (Iliev *et al* 1988, Sendova-Vassileva *et al* 1988) one expects that at low temperatures the laser lines used in our experiments could excite the $^3K_8$, $^5F_3$, $^5F_4$, $^5S_2$ and $^5F_5$ multiplets. In accord with these expectations, four groups of emission lines were observed as shown in table 1. In the last two columns of table 1 the laser lines that excite effectively the corresponding transitions at 18 and 300 K are given. The lines at 20 141 and 20 492 cm^{-1} are not effective at low temperature as their photon energies are too high above the $^5F_4$, $^5S_2$ levels and indirect excitation with the emission of one phonon is impossible. As long as two new ways of excitation become possible at room temperature, namely, from these higher components of the ground multiplet and with the absorption of one phonon, these lines start to excite the $^5F_3$ multiplet and, by radiationless transition, the $^5F_4$, $^5S_2$ and $^5F_5$ multiplets.

Table 1. Main groups of lines in the laser excited luminescence of CaF_2: Ho.

Spectral region cm^{-1}	Transition	Effective laser lines cm^{-1}	
		18 K	300 K
20800–20100	$^5F_3 \rightarrow {}^5I_8$	20987	20987 20492
19100–17700	$^5F_4, {}^5S_2 \rightarrow {}^5I_8$	20987 19435	21837 20987 20492 20141 19435
15800–14900	$^5F_3 \rightarrow {}^5I_7$	20987	20987 20492
	$^5F_5 \rightarrow {}^5I_8$	20987 15802	20987 20492 15802
13700–12900	$^5F_4, {}^5S_2 \rightarrow {}^5I_7$	20987 19435	21837 20987 20492 20141 19435

The number of lines, their relative intensity and their linewidths and positions vary with temperature. As an example figure 2 shows the evolution with temperature of the spectrum in the $^5F_4, {}^5S_2 \rightarrow {}^5I_7$ region.

Using a computer program, sections of the spectra of figure 2 and similar spectra measured at other temperatures were fitted with Lorentzians or Gaussians, or both, or a mixture of both. In this way the linewidth versus temperature changes were obtained for most of the lines. The same was performed for the $^4S_{3/2} \rightarrow {}^4I_{15/2}$ spectra of Er^{3+} in CaF_2: Er reported earlier by Sendova-Vassileva *et al* (1988). Some typical results are given in figures 3 and 4. These were compared with existing theoretical models as will be shown in the next section.

4. Temperature evolution of the linewidths of the $Ho^{3+}(^5F_4, {}^5S_2 \rightarrow {}^5I_7)$ and $Er^{3+}(^4S_{3/2} \rightarrow {}^4I_{15/2})$ luminescence lines

Two different models for the evolution with temperature of the emission linewidths will be explored. The *adiabatic model* (model I) (see e.g. Osad'ko 1979 and Hsu and Skinner 1984) considers the radiation transition between two electronic levels in the harmonic Franck–Condon approximation. The *model of phonon-induced relaxation* (model II) used by Yen *et al* (1964) takes into account the 'direct' one-phonon relaxation between the crystal field components of a level, the radiationless transitions between multiplets and the Raman processes of phonon scattering by impurity ions.

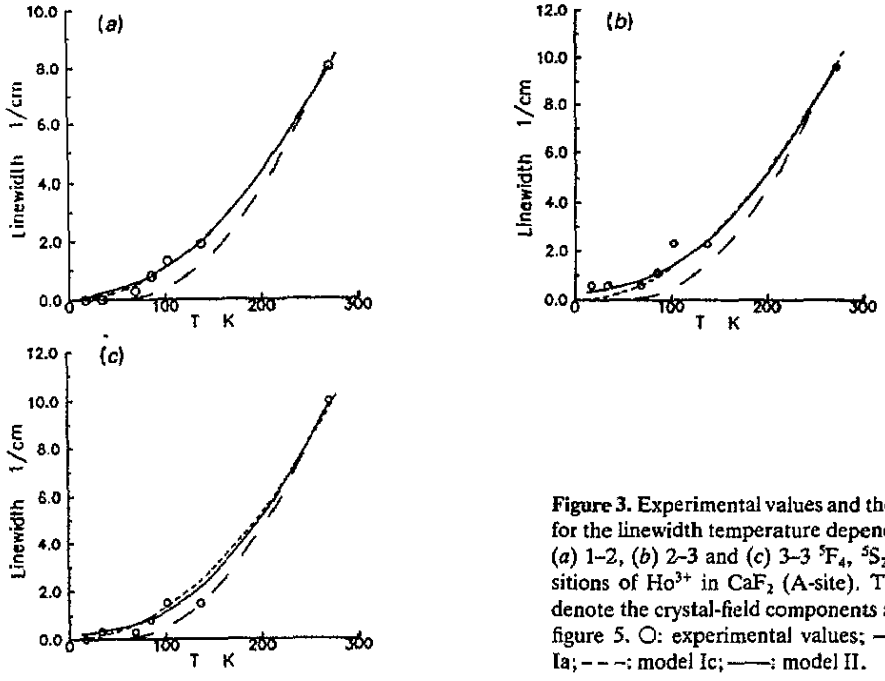

Figure 3. Experimental values and theoretical fits for the linewidth temperature dependence of the (*a*) 1–2, (*b*) 2–3 and (*c*) 3–3 $^5F_4$, $^5S_2 \rightarrow {}^5I_7$ transitions of Ho^{3+} in CaF_2 (A-site). The numbers denote the crystal-field components as shown on figure 5. O: experimental values; — —: model Ia; – – –: model Ic; ——: model II.

Within the framework of model I the expression for the dependence on temperature of the homogeneous linedwidth of the 'no-phonon' line $\gamma(T)$ simplifies provided the relation

$$\Delta\gamma/\Delta T \leqslant 0.05\ \mathrm{cm}^{-1}\ \mathrm{K}^{-1} \tag{1}$$

is satisfied (Osad'ko 1979).

As long as (1) is fulfilled in our case for all the transitions of Ho^{3+} and some of the transitions of Er^{3+} (see figures 3 and 4) the expression for $\gamma(T)$ takes the following forms depending on the form of the phonon density-of-states under consideration (Debye distribution, localized vibration or the weighted density-of-states).

For a Debye distribution (model Ia) one obtains (Osad'ko 1979):

$$\gamma(T) = \nu_D 18\pi b^2 \left(\frac{T}{\theta}\right)^7 \int_0^{\theta/T} \frac{x^6 e^x}{(e^x-1)^2}\,dx = C_1 \left(\frac{T}{\theta}\right)^7 \int_0^{\theta/T} \frac{x^6 e^x}{(e^x-1)^2}\,dx \tag{2}$$

where ν_D and θ are the Debye frequency and Debye temperature, $b = W/\nu_D^2$ is a dimensionless parameter, W being related to the change of the elastic constant in the transition from ground to excited electronic state (Franck–Condon model). The constant $C_1 = 18\pi W^2 \nu_D^{-3}$ is optimized in the fitting procedure.

For localized vibrations with frequency ν_l and halfwidth γ_l (model Ib) one obtains (Osad'ko 1979):

$$\gamma(T) = \frac{W^2}{\nu_l^2 \gamma_l} n(\nu_l)[n(\nu_l)+1] = C_2 n(\nu_l)[n(\nu_l)+1] \tag{3}$$

where $n(\nu_l)$ is the thermal equilibrium phonon population. Both C_2 and ν_l are optimized fitting the experimental points.

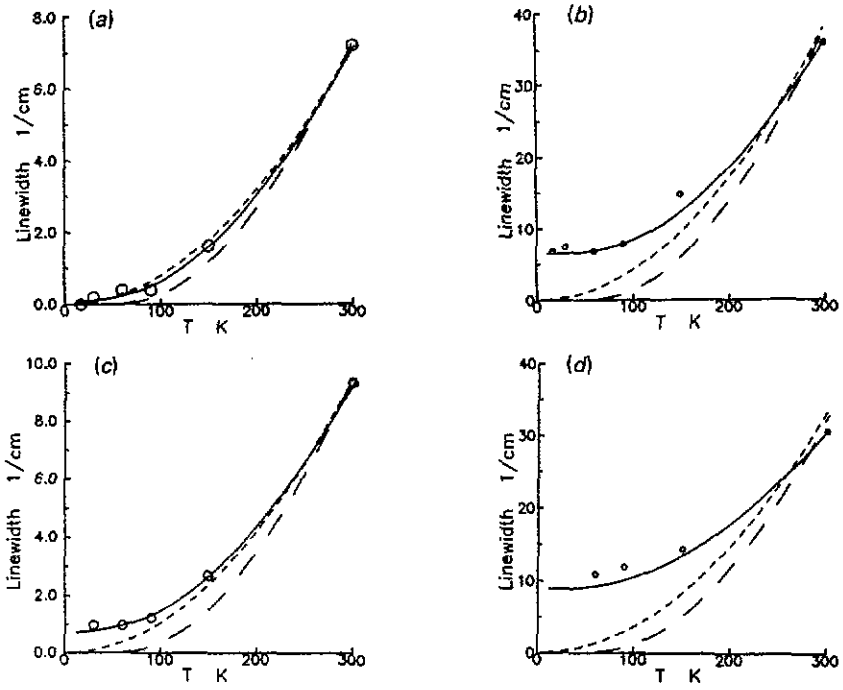

Figure 4. *Experimental values and theoretical fits for the linewidth temperature dependence* of the (*a*) 1–3, (*b*) 1–6, (*c*) 2–2 and (*d*) 2–6 $^4S_{3/2} \rightarrow {}^4I_{15/2}$ transitions of Er^{3+} in CaF_2 (A-site). The numbers denote the crystal-field components as shown in figure 6. O: experimental values, — —: model Ia, – – –: model Ic, ——: model II.

In the model Ic where the weighted density of phonon states of the real crystal $\Gamma(\nu)$ is used, $\gamma(T)$ takes the form (Osad'ko 1979):

$$\gamma(T) = 2\frac{W^2}{\pi}\int_0^\infty \Gamma^2(\nu)n(\nu)[n(\nu)+1]\,\mathrm{d}\nu = C_3\int_0^\infty \Gamma^2(\nu)n(\nu)[n(\nu)+1]\,\mathrm{d}\nu \qquad (4)$$

where C_3 is the fitting parameter. The data for $\Gamma(\nu)$ are those reported by Elcombe and Pryor (1970).

At low temperatures the lines we observe are very narrow and predominantly of Gaussian shape. Following Yen *et al* (1964) we presume that the smallest linewidth observed (0.4 cm^{-1} for the $^5F_4$, $^5S_2 \rightarrow {}^5I_7$ transitions of Ho^{3+} and 1.0 cm^{-1} for the $^4S_{3/2} \rightarrow {}^4I_{15/2}$ transitions of Er^{3+}) is due to temperature-independent inhomogeneous broadening, the latter being the same for all transitions. Using the tables of Posener (1959) the inhomogeneous width was subtracted from the experimental width of the luminescence lines. We note here that the spectral band width of the spectrometer is of the same order of magnitude and may contribute partly to the value of the smallest linewidth.

Figures 3 and 4 show the experimentally measured values of the homogeneous linewidths of some emission lines at various temperatures and the fits the models provide. One finds that model Ic provides a systematically better fit than model Ia. Model Ib (not shown on the figures) is sometimes as good as model Ic but it optimizes two parameters.

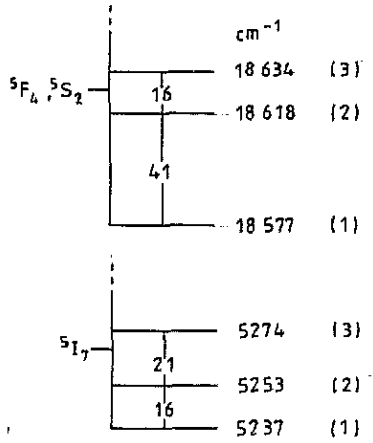

Figure 5. Energy level scheme of Ho^{3+} A-site for model II.

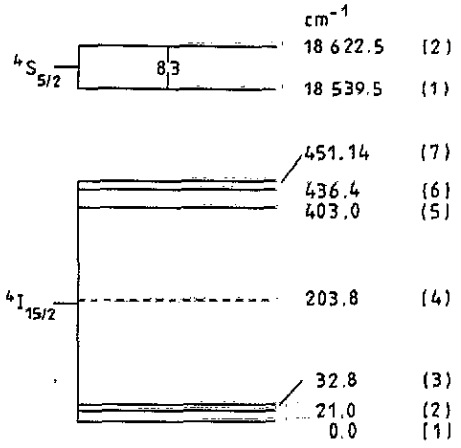

Figure 6. Energy level scheme of Er^{3+} A-site for model II.

Figures 3(*b*) and 4(*b*)–(*d*) as well as the experimental data for some other lines (not included here) show that at low temperatures the theoretical curve corresponding to model Ic deviates from the experimental points. The experimental values are greater than expected and the 0 K intercepts of the linewidth curves are not zero. In fact, for the transitions 1–5, 1–6, 1–7, 2–5 and 2–6 of Er^{3+} the simplified form of model I is not applicable as the condition (1) is not fulfilled. It should be noted that model II can account for this non-zero 0 K intercept if either the starting or the final level of the radiation transition is not the lowest level of the multiplet. In that case even at 0 K there is a possibility for one-phonon relaxation from that level to lower ones within the multiplet, i.e. for phonon induced line broadening.

In order to apply model II the energy differences between the crystal field components of the multiplets have to be known. In the case of Er^{3+} at A-sites the energies of these components are well known (Tallant and Wright 1975). As for Ho^{3+}, the sublevel energies within the multiplets are not firmly established. We used the absorption and emission data of Seelbinder and Wright (1979) supposing that the energies of the three lowest absorption lines of the $^5I_8 \rightarrow {}^5F_4$, $^5S_2$ transition at A-site correspond to the energies of the lowest three sublevels of the $^5F_4$, $^5S_2$ multiplet. In the same manner we assume that the three emission lines highest in energy related to the $^5F_4$, $^5S_2 \rightarrow {}^5I_7$ transition start from the lowest sublevel of the $^5F_4$, $^5S_2$ multiplet and end on the three lowest sublevels of the $^5I_7$ multiplet. Both assumptions are reasonable as the spectra have been taken at 4.2 K and, hence, except for the lowest one, the populations of all sublevels within the ground and excited multiplets could be neglected. In this way the energy level diagram of A-site Ho^{3+} was obtained (figure 5) and further used to obtain the expressions for model II. The curves representing model II in figure 3 are described by

$$\Delta\gamma_{1\text{-}2} = 0.23\,n(41) + 0.24\,n(57) + 0.09\,[n(16) + 1] + 112\,(T/\theta)^7\,\xi_6(\theta/T) \tag{5}$$

$$\Delta\gamma_{2\text{-}3} = 0.23\,[n(41) + 1] + 0.13\,[n(37) + 1] + 166\,(T/\theta)^7\,\xi_6(\theta/T) \tag{6}$$

$$\Delta\gamma_{3\text{-}3} = 0.24\,[n(57) + 1] + 0.13\,[n(37) + 1] + 176\,(T/\theta)^7\,\xi_6(\theta/T) \tag{7}$$

where $n(N)$ is the thermal equilibrium population of the phonon states with energy corresponding to $N\,\mathrm{cm}^{-1}$ and $\xi_6(\theta/T)$ is the Ziman integral $\int_0^{\theta/T} [x^6 e^x/(e^x-1)^2]\,dx$.

The energy level diagram for the A-site $^4S_{3/2} \rightarrow {}^4I_{15/2}$ transitions of Er^{3+} is given in figure 6. In order to reduce the number of parameters in model II and to verify the qualitative explanation given by Sendova-Vassileva *et al* (1988) the emission lines were divided into two groups. The first group consists of the lines ending on the lower three sublevels of the $^4I_{15/2}$ multiplet whereas the second group includes those lines which end on the upper three components of the same multiplet. For the first group of lines, model II is applied in a similar way to that used for Ho^{3+} ignoring the upper three components of $^4I_{15/2}$ as they are much higher in energy. The fitting curves for the lines of figures 4(*a*) and 4(*c*) are:

$$\Delta\gamma_{1\text{-}3} = 0.61\,n(83) + 0.089\,[n(53)+1] + 93\,(T/\theta)^7\,\xi_6(\theta/T) \tag{8}$$

$$\Delta\gamma_{2\text{-}2} = 0.61\,[n(83)+1] + 0.094\,[n(21)+1] + 109\,(T/\theta)^7\,\xi_6(\theta/T). \tag{9}$$

For the second group all the one-phonon relaxations within the ground multiplet are ignored except for the ones between the upper three and the lower three sublevels. For simplicity we presume that such relaxation takes place by the emission of one phonon of $\approx 400\,\mathrm{cm}^{-1}$. That greatly reduces the number of parameters and underlines the importance of this particular relaxation with the emission of higher-energy phonons. Thus the curves corresponding to model II in figures 4(*b*) and 4(*d*) follow the expressions:

$$\Delta\gamma_{1\text{-}6} = 2.4\,n(83) + 6.48\,[n(400)+1] + 398\,(T/\theta)^7\,\xi_6(\theta/T) \tag{10}$$

$$\Delta\gamma_{2\text{-}6} = 2.4\,[n(83)+1] + 6.48\,[n(400)+1] + 268\,(T/\theta)^7\,\xi_6(\theta/T). \tag{11}$$

5. Discussion

The comparison between the dependencies on T of the experimentally obtained emission linewidths and the ones predicted by model Ia, model Ib, model Ic and model II gives strong evidence that all the lattice phonons of CaF_2 are involved in the electron–phonon interaction at the A-sites in CaF_2:Ho and CaF_2:Er. Indeed the values of ν_l used as a fitting parameter in model Ib vary so much from line to line that it is doubtful that a

Table 2.

Ho^{3+} $^5F_4, {}^5S_2 \rightarrow {}^5I_7$		Er^{3+} $^4S_{3/2} \rightarrow {}^4I_{15/2}$	
Transition	$C_3\,(\mu\mathrm{m}^{-6}\,\mathrm{s}^2)$	Transition	$C_3\,(\mu\mathrm{m}^{-6}\,\mathrm{s}^2)$
1–1	30	1–1	22
1–2	24	1–2	17
1–3	28	1–3	18
2–1	18	2–2	24
2–3	34	2–3	16
3–2	14	—	—
3–3	22	—	—

single localized vibration could be responsible for the broadening of these lines. On the other hand, the fit of model Ic is very good, keeping in mind that only one parameter is optimized.

The values of C_3 for some transitions for which the linewidth versus T dependence is well fitted within the framework of model Ic are given in table 2. The C_3 values are of the same order of magnitude for both Ho^{3+} and Er^{3+} and one can draw the conclusion that the second-order adiabatic electron–phonon interaction is comparable for these two ions.

Model II gives a relatively good fit both for the lines for which model Ic is appropriate and for most of the rest of the lines. The mechanism of one-phonon relaxation between the crystal field components of a multiplet is undoubtedly significant for the thermal broadening of the rare-earth luminescence lines. A proof of this is the good fit for the Er^{3+} linewidths in spite of the simplified versions of the employed model. These results are completely in line with the earlier qualitative explanation of the differing widths of the Er^{3+} emission lines proposed by Sendova-Vassileva *et al* (1988).

References

Elcombe M M and Pryor A W 1970 *J. Phys. C: Solid State Phys.* **3** 492
Erickson L E 1975 *Opt. Commun.* **15** 246
Hsu D and Skinner J L 1984 *J. Chem. Phys.* **81** 1604
Iliev M, Liarokapis E and Sendova M Bl 1988 *Phys. Chem. Mineral.* **15** 597
Osad'ko I S 1979 *Usp. Fiz. Nauk.* **128** 31
Posener D W 1959 *Aust. J. Phys.* **12** 184
Seelbinder M B and Wright J C 1979 *Phys. Rev.* B **20** 1308
Sendova-Vassileva M, Iliev M and Liarokapis E 1988 *Bulg. J. Phys.* **4** 367
Tallant D R and Wright J C 1975 *J. Chem. Phys.* **63** 2074
Yen W M, Scott W C and Schawlow A L 1964 *Phys. Rev.* **136** A271